Green fluorescent protein-like pigments optimize the internal light environment in symbiotic reef building corals

Elena Bollati[1,2,3*], Niclas H. Lyndby[2,4], Cecilia D'Angelo[1], Michael Kühl[2,5], Jörg Wiedenmann[1] & Daniel Wangpraseurt[6,7,8*]

[1]Coral Reef Laboratory, School of Ocean and Earth Science, University of Southampton, United Kingdom

[2]Marine Biology Section, Department of Biology, University of Copenhagen, Strandpromenaden 5, DK-3000 Helsingør, Denmark

[3]Department of Biological Sciences, National University of Singapore, 16 Science Drive 4, Singapore 117558

[4]Laboratory for Biological Geochemistry, School of Architecture, Civil and Environmental Engineering, Ecole Polytechnique Fédérale de Lausanne (EPFL), CH-1015 Lausanne, Switzerland

[5]Climate Change Cluster, University of Technology Sydney, Ultimo, NSW 2007, Australia

[6]Department of NanoEngineering, UC San Diego, USA

[7]Marine Biological Research Division, Scripps Institution of Oceanography, UC San Diego, USA

[8]Bioinspired photonics group, Department of Chemistry, University of Cambridge, UK

*Correspondence: dwangpraseurt@ucsd.edu, elena.bollati@bio.ku.dk

Short/running title: Host pigments and light microclimate in corals

Keywords: Symbiosis, photobiology, GFP, optics, fluorescence, photoconversion

Abstract

Pigments homologous to the Green Fluorescent Protein (GFP) have been proposed to fine-tune the internal light microclimate of corals, facilitating photoacclimation of photosynthetic coral symbionts (Symbiodiniaceae) to life in different reef habitats and environmental conditions. However, direct measurements of the *in vivo* light conditions inside the coral tissue supporting this conclusion are lacking. Here, we quantified the intra-tissue spectral light environment of corals expressing GFP-like proteins from widely different light regimes. We focus on (1) photoconvertible red fluorescent proteins (pcRFPs), thought to enhance photosynthesis in mesophotic habitats via wavelength conversion, and (2) chromoproteins (CPs), which provide photoprotection to the symbionts in shallow water via light absorption. Optical microsensor measurements indicated that both pigment groups strongly alter the coral tissue light environment. Estimates derived from light spectra measured in pcRFP-containing corals showed that fluorescence emission can contribute to >50% of orange-red light available to the photosynthetic symbionts at mesophotic depths. We further show that upregulation of pink CPs in shallow-water corals during bleaching leads to a reduction of orange light by 10-20% compared to low-CP tissue. Thus, screening by CPs has an important role in mitigating the light-enhancing effect of coral tissue scattering during bleaching. Our results provide the first experimental quantification of the importance of GFP-like proteins in fine-tuning the light microclimate of corals during photoacclimation.

Introduction

Tropical coral reefs are solar-powered oases of marine biodiversity, where scleractinian corals are responsible for building the reef structures that host over 30% of all named marine multicellular species (Fisher et al. 2015). Corals rely heavily on photosynthesis by their dinoflagellate endosymbionts (Symbiodiniaceae) to meet their metabolic requirements (Muscatine 1990). The distribution of reef-building corals is therefore constrained by the availability of photosynthetically active radiation (PAR, 400-700 nm), which is in turn determined by physical factors such as latitude, seasonality, water depth and the optical properties of the water body (Kirk 1994; Kleypas et al. 1999; López-Londoño et al. 2021). Variability in these parameters affects both the quantity and spectral quality of irradiance, exposing corals to a large range of light environments even across small spatial scales (Brakel 1979; Anthony and Hoegh-Guldberg 2003; Eyal et al. 2015). On shallow reef flats in clear water regions, corals are routinely exposed to excess irradiance that supersaturates symbiont photosynthesis (Jimenez et al. 2012; Wangpraseurt et al. 2014b), with short light flashes reaching over 3900 µmol photons m^{-2} s^{-1} due to the lensing effect of waves (Veal et al. 2010). Additionally, shallow water corals are exposed to a broad irradiance spectrum covering ultraviolet (UV) to near infrared (NIR) radiation (Wangpraseurt et al. 2014b). At the other

extreme, photosynthetic corals on mesophotic reefs at water depths between 50-150 m can receive as little as 1% of surface PAR, largely concentrated in the blue-green region of the spectrum and greatly reduced for UV and red wavebands (Lesser et al. 2009; Eyal et al. 2015; Tamir et al. 2019). Light conditions can also vary for individual colonies from the same water depth depending on colony morphology (Kaniewska et al. 2011; Wangpraseurt et al. 2014b) and the reef structure that surrounds them (Falkowski and Dubinsky 1981; Wangpraseurt et al. 2014b).

Corals have evolved a number of mechanisms for optimising symbiont photosynthesis in the presence of spatial and temporal heterogeneity in light availability. Some of these mechanisms occur at the symbiont cell level, while others involve changes in coral host morphology both at the colony and polyp-scale (Kramer et al.; Hoogenboom et al. 2008; Todd 2008). Coral symbionts can modify their light harvesting and energy quenching over timescales ranging from seconds to months. For example, non-photochemical quenching allows rapid dissipation of excess irradiance in the photosynthetic apparatus of symbionts, preventing photodamage in high light environments (Hoegh-Guldberg and Jones 1999; Gorbunov et al. 2001). Changes in photosynthetic pigment concentrations and symbiont cell numbers enable corals to acclimate to changes in irradiance over longer time periods (Falkowski and Dubinsky 1981; Titlyanov et al. 2001); specifically, corals can increase their symbiont numbers as well as the per cell photosynthetic pigment content in response to a reduction in light levels, and vice versa (Falkowski and Dubinsky 1981; Titlyanov et al. 2001).

Coral host morphology is an important factor controlling the irradiance available for symbiont photosynthesis (Helmuth et al. 1997; Ralph et al. 2002; Einbinder et al. 2009; Kaniewska et al. 2011; Nir et al. 2011; Wangpraseurt et al. 2014b; Kahng et al. 2019). Coral colonies from low light environments maximize their interception with the downwelling irradiance and assume plate-like morphologies that are more conducive to light gathering, while shallow water colonies assume more self-shading morphologies, such as vertical plates or branches (Anthony et al. 2005; Kaniewska et al. 2011). Morphological adaptations make some species depth-specialists, such as the mesophotic coral *Leptoseris* which can host photosynthetic symbionts down to depths of well over 100 m (Rouzé et al. 2021). Growth form can also exhibit a great degree of phenotypic plasticity in many coral species, as evident from changes in morphology when colonies are transplanted across depth gradients (Willis 1985; Tamir et al. 2020). Such plasticity is one of the factors that enables depth generalist corals, such as *Montastraea cavernosa* in the Caribbean, to thrive across light gradients of several orders of magnitude (Lesser et al. 2010).

Light availability to the coral symbionts depends on the optical properties of the surrounding host tissue and the underlying skeleton (Wangpraseurt et al. 2012, 2019; Marcelino et al. 2013). Coral tissue and skeleton scatter incident light with a strength and directionality that

are highly variable across species and even between different structures within a single colony (Marcelino et al. 2013; Wangpraseurt et al. 2016a, 2019; Enríquez et al. 2017). The interplay between tissue and skeleton scattering and reflection and algal absorption modulate coral photosynthesis (Marcelino et al. 2013; Brodersen et al. 2014; Wangpraseurt et al. 2016a, 2019; Scheufen et al. 2017). In some corals, this can lead to outstanding photosynthetic quantum efficiencies that are close to the theoretical maximum (Brodersen et al. 2014). Optical properties of coral colonies exhibit ontogenetic plasticity, which enables some coral species to occupy a wider niche (Anthony et al. 2005). For example, on mesophotic reefs the depth-generalist corals *Paramontastrea peresi* and *Porites lobata* tend to assume growth forms with enhanced light exposure and skeletons with higher reflectivity compared to their shallow water conspecifics, resulting in higher absorption by the symbionts (Kramer et al. 2020).

The coral host can also modulate incident light by synthesizing host pigments. The most widespread coral host pigments belong to the Green Fluorescent Protein (GFP)-like superfamily, a group of homologous pigments which are ubiquitous among the Cnidaria (Shimomura et al. 1962; Matz et al. 1999; Alieva et al. 2008). Pigments in this family share a similar structure based on a tripeptide chromophore capable of absorbing visible or UV radiation (Nienhaus and Wiedenmann 2009). However, despite having similar structure, cnidarian GFP-like proteins exhibit great variability in their optical properties and regulation mechanisms, indicating that they are functionally diverse (Salih et al. 2000; Leutenegger et al. 2007; Alieva et al. 2008; D'Angelo et al. 2008; Nienhaus and Wiedenmann 2009; Smith et al. 2013; Aihara et al. 2019).

GFP-like proteins with inducible expression are found predominantly in corals from high light environments, and they are transcriptionally regulated by blue light intensity (Salih et al. 2000; D'Angelo et al. 2008). GFP-like proteins with light-induced expression include fluorescent proteins (FPs) with emission in the cyan, green and red spectral regions (CFPs, GFPs and RFPs), which absorb light and re-emit it as red-shifted radiation, and non-fluorescent chromoproteins (CPs), which absorb light but have no or little fluorescence emission (Alieva et al. 2008; D'Angelo et al. 2008). These pigments accumulate in high concentration in colony parts with low symbiont densities, often areas of active growth, such as skeletal ridges, the tips of branching corals, the margins of plating corals, and areas affected by epibionts and mechanical damage (Salih et al. 2000; D'Angelo et al. 2012). The increased photon fluxes inside the host tissue caused by the absence of light absorption by the symbionts and light reflection and scattering by skeleton and host tissue components (Enríquez et al. 2005; Wangpraseurt et al. 2017) have been suggested to cause the high-level pigment expression in these colony parts (Smith et al. 2013; Bollati et al. 2020). Additionally, blue light-induced upregulation as part of an optical feedback loop has been shown to drive strong accumulation

139 of these pigments in bleached corals during episodes of mild heat stress or in heat-free
140 bleaching, caused, for instance, by nutrient stress (Bollati et al. 2020).
141 FPs and CPs with light-induced expression are usually localised ectodermally, and have been
142 shown to exert a photoprotective function on the underlying symbiont layer (Salih et al. 2000;
143 Smith et al. 2013; Gittins et al. 2015; Quick et al. 2018). Upregulation of these pigments in
144 growing parts of colonies and in bleached tissue has been proposed to promote
145 (re)colonisation of host tissue by symbiont cells via the reduction of internal light stress in
146 areas with low symbiont densities (D'Angelo et al. 2012; Smith et al. 2013; Bollati et al. 2020).
147 GFP-like proteins are also widely distributed in corals that are depth generalists or even
148 mesophotic specialists (Oswald et al. 2007; Eyal et al. 2015), where they are constitutively
149 expressed, often at high levels, across a wide range of irradiance regimes (Leutenegger et al.
150 2007). It has long been proposed that fluorescent pigments in low light habitats could enhance
151 coral photosynthesis by modulating the spectrum and intensity of light that reaches the
152 symbiont cells (Schlichter et al. 1994; Salih et al. 2000). A light-enhancement mechanism has
153 been suggested for a particular group of constitutive GFP-like proteins known as
154 photoconvertible RFPs (pcRFPs), which are common in thick-tissue depth generalist and
155 mesophotic coral species (Ando et al. 2002; Wiedenmann et al. 2004; Oswald et al. 2007;
156 Eyal et al. 2015). pcRFPs emit green fluorescence when first synthesised, but their
157 chromophores are irreversibly converted to a red-emitting species upon absorption of a UV
158 photon ~390 nm (Ando et al. 2002; Wiedenmann et al. 2004). As coral GFP-like proteins are
159 typically arranged in tetramers, UV-induced post-translational modification leads to the
160 formation of tetramers that contain both green and red subunits; they can therefore absorb
161 light in the blue-green range and re-emit it in the orange-red range via highly efficient Förster
162 Resonance Energy Transfer (FRET) between adjacent subunits (Wiedenmann et al. 2004;
163 Bollati et al. 2017). The orange-red waveband is scarce on mesophotic reefs, yet it can
164 stimulate chlorophyll fluorescence deeper in the tissue compared to blue-green wavelengths
165 because it is poorly absorbed by photosynthetic pigments, an effect analogous to green light
166 driven photosynthesis in plant leaves (Vogelmann and Evans 2002; de Mooij et al. 2016; Smith
167 et al. 2017). Indeed, pcRFP-containing corals have been shown to survive better under a
168 simulated mesophotic light spectrum as compared to non-pigmented conspecifics (Smith et
169 al. 2017).
170 While GFP-like proteins are likely to have additional functions for the coral holobiont (Aihara
171 et al. 2019; Id et al. 2021), optimisation of the symbiont light environment is arguably one of
172 their primary roles. The effects of GFP-like proteins on the light environment experienced by
173 coral symbionts are not simply dependent on the spectral properties of the isolated protein;
174 rather, they are a product of the environmental and physiological regulation of the protein
175 within its three-dimensional optical context. For example, microsensor measurements and

176 optical modelling have shown that scattering by GFP-like proteins can enhance light
177 penetration at low GFP concentrations, while high concentrations of GFP increase
178 backscattering and reduce light penetration through the coral tissue (Lyndby et al. 2016;
179 Parkins et al. 2021). Variability in the distribution and arrangement of these proteins – diffuse
180 or granular, ectodermal or endodermal – also affects how they interact with light (Salih et al.
181 2000; Wangpraseurt et al. 2019), further indicating that spectrally similar GFP-like proteins
182 can be involved in different light modulation mechanisms.
183 Studies examining the *in vivo* internal light environment of coral colonies at the microscale,
184 particularly during environmentally driven changes in their GFP-like protein complement, are
185 therefore an essential step towards understanding the role these proteins play in
186 photoacclimation of symbiotic corals. Here, we investigated how environmental regulation of
187 GFP-like proteins affects the intra-tissue light microenvironment of depth-generalist and
188 shallow water corals. We focused on the effects of i) UV-driven photoconversion in corals
189 containing pcRFPs, and ii) blue light-driven upregulation of inducible CPs during bleaching
190 and in active growth colony margins. Our study provides direct evidence for the importance of
191 GFP in optimizing the coral-algal symbiosis under extreme light regimes.
192
193 **Results and Discussion**
194 Photoconversion and pcRFPs in depth generalist corals
195 Measurements of scalar irradiance taken at the tissue surface of *M. cavernosa* under white
196 illumination showed an enhancement of 120-180% of the incident irradiance across the visible
197 spectrum. This enhancement was detected for all specimens regardless of the degree of
198 photoconversion (Fig. 1a). Vertical light attenuation was strongest between 410-470 nm
199 (covering chlorophyll *a* absorption) and weakest in orange-red wavebands (Fig. 1b).

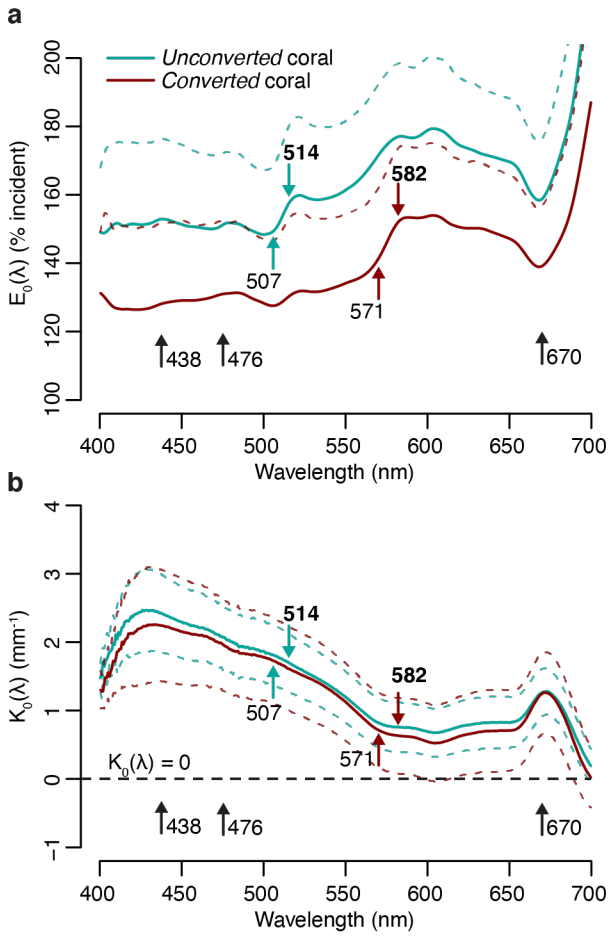

Figure 1. Spectral scalar irradiance in *M. cavernosa* under broad spectrum light. a) $E_0(\lambda)$ at coenosarc surface, with excitation and emission peaks of unconverted and converted McavRFP highlighted (colorful arrows), as well as absorption peaks of Symbiodiniaceae photosynthetic pigments (black arrows). Mean (solid lines) + s.d. (dashed lines); n=3 measurements on 2 fragments. **b**) Spectral attenuation coefficient of $E_0(\lambda)$ from coenosarc surface to skeleton (average thickness = 560 μm). Mean (solid lines) ± s.d. (dashed line), n=3.

The enhancement of scalar irradiance commonly observed at the surface of coral colonies is a result of light scattering by the underlying tissue and skeleton (Kühl et al. 1995; Wangpraseurt et al. 2014a), which displays great interspecific variability (Marcelino et al. 2013; Wangpraseurt et al. 2019). Depending on the scattering strength of the two compartments, light in deeper aboral tissue layers can be strongly reduced (Wangpraseurt et al. 2012) or enhanced (Szabó et al. 2014; Wangpraseurt et al. 2020), relative to the top (oral) tissue layers. Our measurements of the tissue attenuation coefficient for *M. cavernosa* indicate shading of the deeper tissue areas, particularly in the violet-blue range (Fig. 1b). Additionally, previous measurements of optical scattering suggest that light enhancement due to skeleton backscatter is limited for this species compared to other coral taxa (Marcelino et al. 2013). While these properties may confer bleaching resistance and provide photoprotection for the symbiont population in shallow water (Wangpraseurt et al. 2012; Marcelino et al. 2013), tissue

221 shading greatly reduces carbon fixation rates in symbiont cells found in deeper tissue layers
222 (Wangpraseurt et al. 2016b), which might negatively affect colonies in light-limited
223 environments; yet, *M. cavernosa* is able to thrive at mesophotic depths (Lesser et al. 2010).
224 At the coral surface, spectral changes due to conversion of the pcRFP pool were observed at
225 the absorption and emission peaks of the green (507 and 514 nm) and red chromophore (571
226 and 582 nm) (Fig. 1a). Surface light enhancement by GFP-like proteins in corals can be
227 attributed to a combination of elastic scattering (i.e. scattering without modifications of photon
228 energy) and inelastic scattering (i.e. scattering with modification of photon energy, such as the
229 case of absorption followed by fluorescence emission) (Lyndby et al. 2016). Under white light,
230 the degree of photoconversion of the pcRFP pool did not appear to significantly affect the
231 spectral attenuation coefficient (Fig. 1b), indicating that the effects of pcRFP scattering on
232 attenuation of the incident are relatively small compared to the effects of tissue scattering and
233 photosynthetic pigment absorption. Host pigment-derived enhancement of light in pcRFP-
234 containing corals in shallow water environments therefore appears a minor component for the
235 overall tissue light microclimate, albeit with some variability due to water depth and the optical
236 properties of the water column, as well as spectral differences between our white measuring
237 light and sunlight. In contrast, corals on mesophotic reefs experience a much more narrow
238 incident spectrum, where blue-green wavelengths that efficiently excite pcRFPs are abundant,
239 while light in the orange-red spectral range is greatly reduced (Lesser et al. 2009; Eyal et al.
240 2015; Tamir et al. 2019). Under these conditions, the relative contributions of light scattering
241 and fluorescence emission by pcRFPs are therefore likely very different from those measured
242 under white light.
243 To isolate the contribution of fluorescence emission by the pcRFP pool to the tissue light
244 microenvironment of *M. cavernosa*, we collected fluorescence emission profiles in the 505-
245 700 nm range using a blue (455-505 nm) excitation light source (Fig. 2, Fig. S1). At all stages
246 of photoconversion (signified by the decreasing 514:582 nm emission ratio and defined as
247 *unconverted*, *partially converted* and *converted*, Fig. 2a,b), fluorescence emission from both
248 the unconverted and converted chromophore was highest at the surface and decreased
249 towards the skeleton. However, attenuation of light emitted by the unconverted chromophore
250 was more pronounced relative to attenuation of the converted chromophore emission (Fig.
251 2a,c). This is in agreement with the white light attenuation coefficient (Fig. 1b), which was
252 weaker in the orange-red range. The peridinin-chlorophyll *a*-protein (PCP) light harvesting
253 complex efficiently absorbs blue, green and red wavelengths (Jiang et al. 2012), resulting in
254 strong attenuation by symbionts in the oral gastrodermis (Fig. 1); conversely, poor absorption
255 of orange light by symbiont pigments allows this waveband to penetrate deeper into the tissue
256 (Fig. 1).

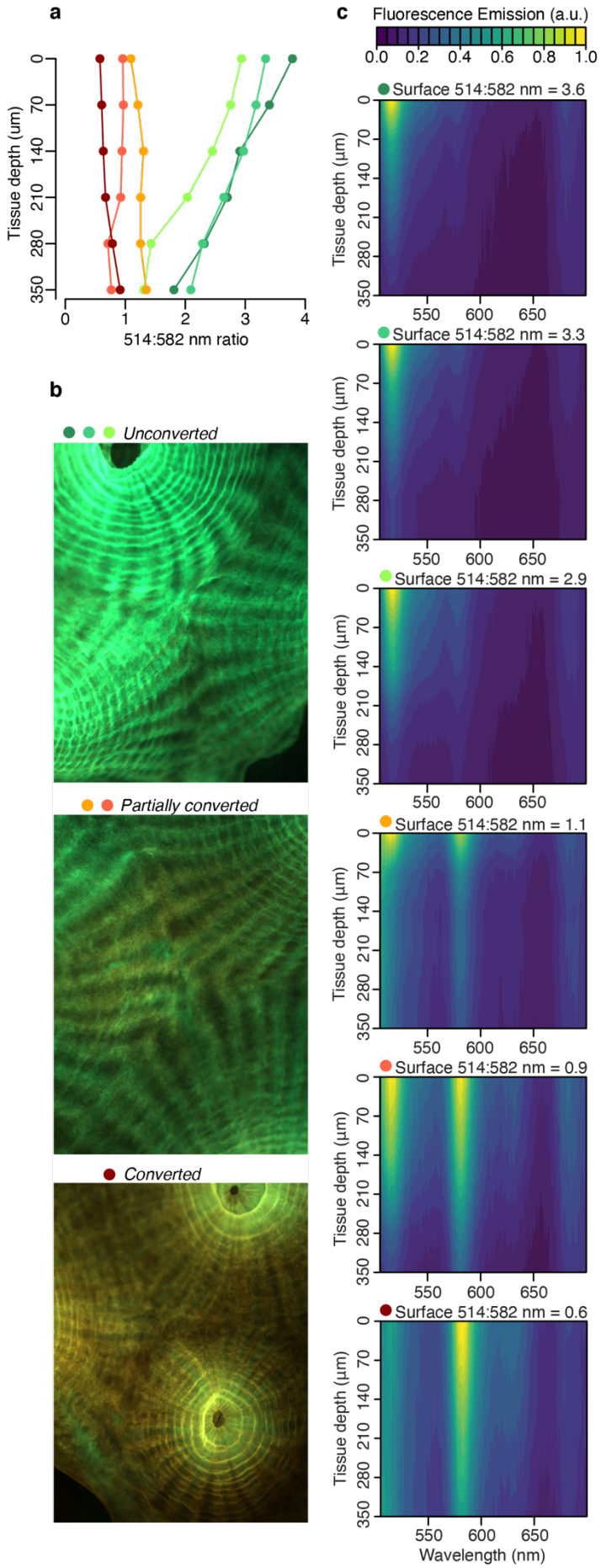
a
Tissue depth (um)
0
70
140
210
280
350
0
1
2
3
4
514:582 nm ratio
b
Unconverted
Partially converted
Converted
c
Fluorescence Emission (a.u.)
0.0
0.2
0.4
0.6
0.8
1.0
Surface 514:582 nm = 3.6
Surface 514:582 nm = 3.3
Surface 514:582 nm = 2.9
Surface 514:582 nm = 1.1
Surface 514:582 nm = 0.9
Surface 514:582 nm = 0.6
Tissue depth (µm)
550
600
650
Wavelength (nm)

Figure 2. Host pigment fluorescence distribution in the tissue of *M. cavernosa* undergoing photoconversion. Scalar irradiance measurements collected under blue excitation 455-505 nm (Fig. S1c). **a**) 514:582 nm emission ratio, indicating the degree of photoconversion for each coral (*unconverted* >1, *partially converted* ~1, *converted* <1). **b**) Fluorescence micrographs of representative photoconversion stages. **c**) Normalised fluorescence emission profiles (arbitrary units, a.u.).

Smith et al. (2017) showed that orange light has a higher potential to stimulate photosynthesis in symbiont cells found deeper in the coral tissue as compared to blue-green light. This effect is analogous to what is observed in plant leaves, where enhanced illumination with green light increases photosynthesis in deeper cell layers (Vogelmann and Evans 2002; de Mooij et al. 2016). Therefore, it was proposed that orange fluorescence emission by pcRFPs could provide an energetic advantage for symbiotic corals in greater water depths dominated by blue light (Smith et al. 2017) Indeed, colour morphs with pcRFPs survived longer than non-pigmented conspecifics in simulated deep water light environments (Smith et al. 2017). Here, we directly quantified the impact of pcRFPs on the light environment experienced by deep symbionts *in hospite* in corals. We used the blue light excited fluorescence emission profiles from *M. cavernosa* (Fig. 2c) at different stages of photoconversion (Fig. 3a-c) to calculate the number of photons generated by fluorescence emission integrated over the green (Fig. 3d) and red (Fig. 3e) spectral range. Fluorescence emission by a converted pcRFP pool provides an amount of orange-red photons that ranges between 1% (close to the skeleton) and 5% (at the coral surface) of the blue incident intensity, with intermediate values of around 3% at a tissue depth of 400 μm (Fig. 3e). This is a more than three times higher contribution by the converted pcRFP, as compared to measurements in the same waveband on *unconverted* coral. Our direct measurements of the coral tissue light field thus provide experimental proof that orange-red fluorescence from host pigments penetrates coral tissues better than green fluorescence, and that ectodermal pcRFPs can improve the illumination of otherwise shaded tissue areas despite the narrow mesophotic light spectrum. Thus, under a mesophotic light spectrum, the symbionts harboured by conspecific fluorescent morphs experience a spectrally different light environment depending on the pigment complement expressed by their host (Ben-Zvi et al. 2021). We obtained a similar result for a second species, *Echinophyllia* sp., by comparing specimens that contain a highly converted pcRFP to conspecific morphs that lack pcRFPs entirely (Fig. S3). This confirms the relevance of our findings to other pcRFP-containing corals from mesophotic environments (Eyal et al. 2015).

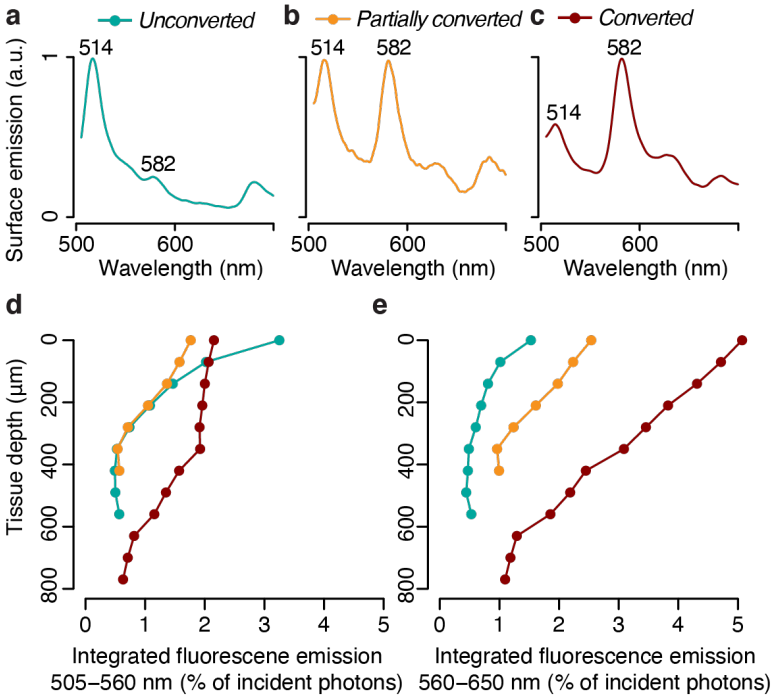

Figure 3. Photon scalar irradiance of host pigment fluorescence in the tissue of *M. cavernosa* at representative photoconversion stages. a) Tissue surface emission spectra of *unconverted*, *partially converted* and *converted* specimens (ex = 455-505 nm). **b**) Integrated green (505-560 nm) and red (560-650 nm) fluorescence emission along a tissue depth profile, measured under blue excitation (455-505 nm, Fig. S1c).

To predict how spectral modifications by pcRFPs affect *in situ* light harvesting on mesophotic reefs, we used a published dataset of downwelling spectral irradiance from a coral reef in Eilat (Eyal et al. 2015) (Fig. 4a) and simulated the *in vivo* emission of orange-red light along a depth gradient from 10 to 130 m, using the *converted M. cavernosa* as a model (Fig. 4b). The incident 455-505 nm light required to excite the pcRFP pool is relatively abundant down to 100 m water depth (1.5 µmol photos m^{-2} s^{-1}), however the amount of 560-650 nm light is only in the range of 1 µmol photons m^{-2} s^{-1} at 50 m and attenuates rapidly to about 0.1 µmol photons m^{-2} s^{-1} at 80 m (Fig. 4a). As a consequence, the pcRFP pool between 50 and 80 m depth can provide at least as many 560-650 nm photons as incident sunlight, effectively doubling the scalar irradiance in this waveband compared to corals without pcRFPs (Fig. 4b). On mesophotic reefs beyond 80 m water depth, fluorescence emission by the pcRFP becomes the dominant source of 560-650 nm light for *M. cavernosa*. This calculation yielded similar results when applied to a dataset of modelled irradiance in the Bahamas (Lesser et al. 2009) (Fig. S4), a natural habitat of this species, suggesting that our findings are relevant to mesophotic reef systems independent from potential differences in the underwater light environment.

We note that our analysis could lead to overestimation of predicted red fluorescence at shallow depths, where high light levels may saturate the chromophore population thus resulting in a

317 non-linear relationship between incident light and fluorescence emission. However, the
318 relationship between fluorescence emission and excitation light was linear up to at least 20
319 μmol photons m^{-2} s^{-1} (of incident 455-505 nm light) (Fig. S5, Table S1), corresponding to the
320 incident irradiance (455-505 nm) measured at 48 m depth in the Red Sea (Fig. 4a). Our
321 calculations of fluorescence emission were thus considered accurate below 48 m water depth.

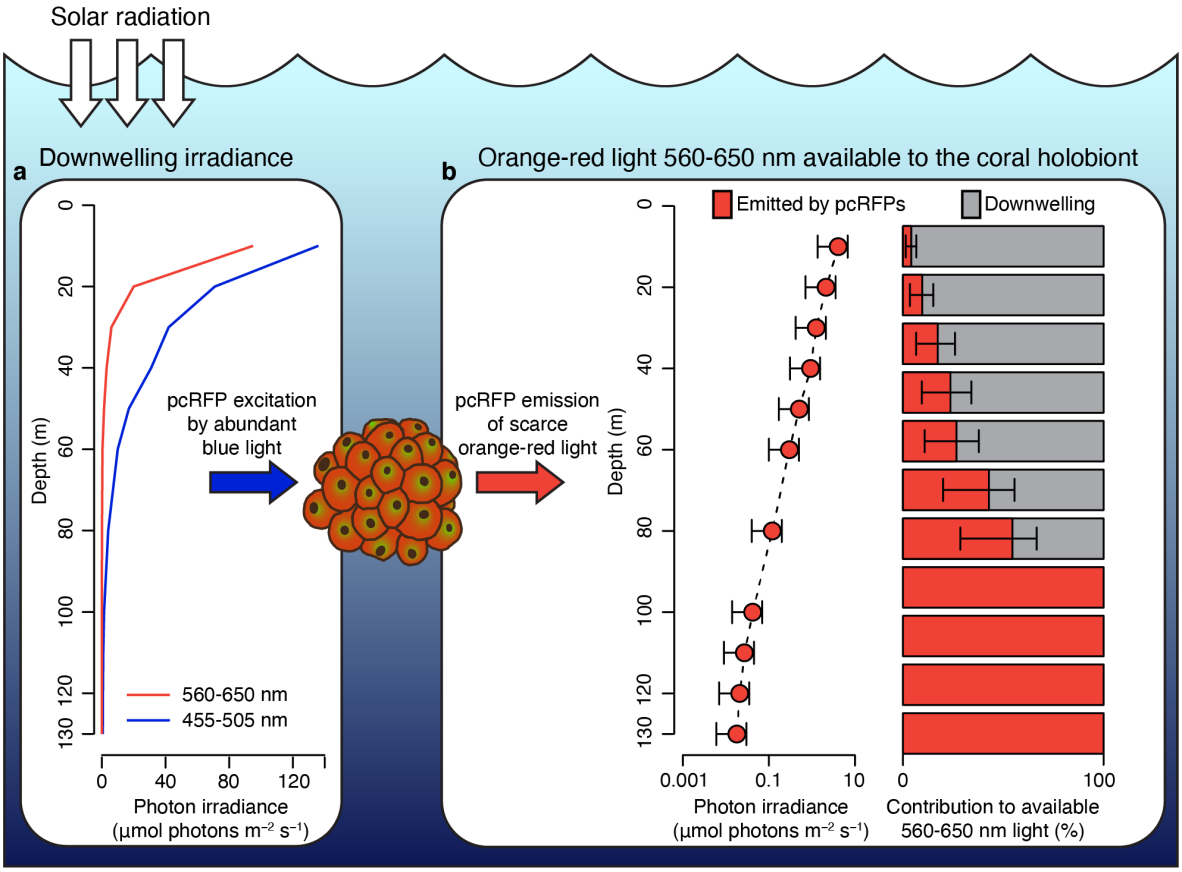

322

323 **Figure 4. Spectral photon irradiance and wavelength conversion in corals with photo-**
324 **convertible host pigments along a depth gradient. a**) Integrated photon irradiance in the
325 450-505 nm and 560-650 nm range measured on a mesophotic reef in Eilat, Red Sea (Eyal
326 et al. 2015). **b**) Measured 560-650 nm light generated by pcRFP emission and estimated
327 relative contribution to the total amount of 560-650 nm light available to the coral holobiont.
328 Error bars represent range between measurement at the coral skeleton (1%) and
329 measurement at the coral surface (5%).
330
331 Even though this constitutes a dramatic spectral alteration in relative terms, it is important to
332 note that the absolute number of photons generated by pcRFP fluorescence is small
333 compared to what is provided by ambient light in shallow waters. The benefit for coral
334 photosynthesis may thus be negligible under higher light conditions in comparison to the
335 metabolic trade-off of having to maintain a highly concentrated pcRFP pool (Leutenegger et
336 al. 2007; Oswald et al. 2007; Quick et al. 2018). Nonetheless, a small advantage can become
337 significant under strong light-limitation, as shown by the increased long term survival of
338 pcRFP-containing coral morphs compared to their brown conspecific kept side-by-side under

339 a simulated mesophotic spectrum (Smith et al. 2017). Such small fitness advantage could
340 have contributed as a driving factor in some of the multiple instances of convergent evolution
341 of red emitting homologues from green ancestor proteins (Shagin et al. 2004; Ugalde et al.
342 2004; Field et al. 2006; Gittins et al. 2015). Furthermore, the benefits and trade-offs
343 associated with high level expression of pcRFPs may have contributed to the rise of colour
344 morphs among individuals from genera such as *Trachyphyllia, Lobophyllia, Echinophyllia* and
345 *Montastraea* (Field et al. 2006; Oswald et al. 2007; Gittins et al. 2015) as a result of balancing
346 selection as previously suggested for GFP-like proteins in both shallow and deep water corals
347 (Quick et al. 2018).
348
349 Photoprotective chromoproteins and bleaching in shallow water corals
350 To evaluate the effect of high ectodermal concentrations of CPs on the light environment of
351 coral symbionts *in hospite*, we performed spectral scalar irradiance measurements on
352 colonies of *Pocillopora damicornis* and *Montipora foliosa*. Pink colour morphs of *P. damicornis*
353 express a CP with absorption maximum at 565 nm (Dove et al. 1995), which can accumulate
354 in high concentrations following bleaching (Bollati et al. 2020) (Fig. 5a). Brown morphs of this
355 species do not produce detectable amounts of CP (Fig. 5a). The bare white skeleton of *P.*
356 *damicornis* enhanced spectral scalar irradiance by 140-150% across the entire visible
357 spectrum (Fig. 5a). In brown morphs, the enhancement was reduced to <120% in the
358 wavebands corresponding to the absorption peaks of symbiont photosynthetic pigments, while
359 the enhancement remained close to 130% in the orange region of the spectrum (Fig. 5a).
360 Bleached corals expressing high pink CP concentrations experienced a surface light
361 enhancement in the blue spectral region comparable to what was measured over bare
362 skeleton; however, this was reduced to ~123% in the orange waveband corresponding to the
363 absorption peak of the CP (Fig. 5b). Measurements of the spectral attenuation coefficient from
364 colony surface to skeleton showed that brown unbleached tissue is light-attenuating in the
365 blue and red regions of photosynthetic pigment absorption, but light-enhancing in the orange-
366 red region; conversely, blue light is enhanced in bleached pink tissue, while orange light is
367 attenuated (Fig. 5c).
368 *M. foliosa* has several colour morphs, one of which produces high concentrations of a purple
369 CP localised in areas of low symbiont density at the colony margins, while the inner area has
370 low CP content and appears brown (D'Angelo et al. 2012) (Fig. 5d). Measurements of surface
371 spectral scalar irradiance on tissue found in the inner region of the colony showed similar
372 spectral properties to those of brown *P. damicornis* and exhibited 140% light enhancement,
373 which was reduced to 110% in the symbiont photosynthetic pigments absorption wavebands
374 (Fig. 5e). In the high CP area at the colony margin, scalar irradiance showed a strong
375 enhancement (>150%) comparable to what measured for bleached tissue in a CP-free morph

376 (Fig. 5e); however, this was heavily spectrally modified by the presence of the purple CP,
377 which reduced light enhancement by up to 25% within its absorption spectrum compared to
378 other spectral bands (Fig. 5e).
379 The *P. damicornis* skeleton exhibits an intermediate level of microscale fractality and an
380 intermediate scattering coefficient (mass-fractal dimension ~1.75 and reduced scattering
381 coefficient of ~7.5 mm^{-1} (Marcelino et al. 2013)), which implies a relatively efficient
382 redistribution of light over the tissue (Marcelino et al. 2013). While this type of skeletal structure
383 can help healthy corals optimise photosynthesis, during bleaching this can amplify the
384 irradiance increase derived from the loss of photosynthetic pigment absorption (Enríquez et
385 al. 2005; Marcelino et al. 2013; Wangpraseurt et al. 2017). Our data confirms that bleached
386 *P. damicornis* tissue indeed experiences a strongly light enhancing microenvironment,
387 resulting from enhanced skeletal scattering due to reduced tissue absorption (Wangpraseurt
388 et al. 2017). Such strongly enhanced light microhabitat can also be found in healthy corals
389 such as in the growing plate margins of *M. foliosa*, where the symbiont population is less
390 abundant compared to the inner areas (Fig. 5d). While blue light is attenuated in unbleached
391 corals, the absence of symbionts in bleached corals or tissue areas with low symbiont
392 densities (e.g. in areas of active tissue growth), results in the enhancement of blue light
393 possibly leading to transcriptional upregulation of CPs (D'Angelo et al. 2008). This supports
394 the notion that the optical feedback loop is a key mechanism underlying the colourful bleaching
395 phenomenon (Bollati et al. 2020). Our data also shows that high CP concentrations counteract
396 the light-enhancing effects of bleaching within the CP absorption spectrum, as signified by the
397 relative light enhancement measured in bleached corals in the orange region, a waveband
398 known to result in light stress and bleaching for various coral species when provided at high
399 irradiance (Smith et al. 2013; Wijgerde et al. 2014; Quick et al. 2018). Thus, optimisation of
400 the light microenvironment by CPs in symbiont-depleted tissue could provide the necessary
401 conditions for (re) colonisation by symbiont cells (D'Angelo et al. 2012; Smith et al. 2013;
402 Bollati et al. 2020).

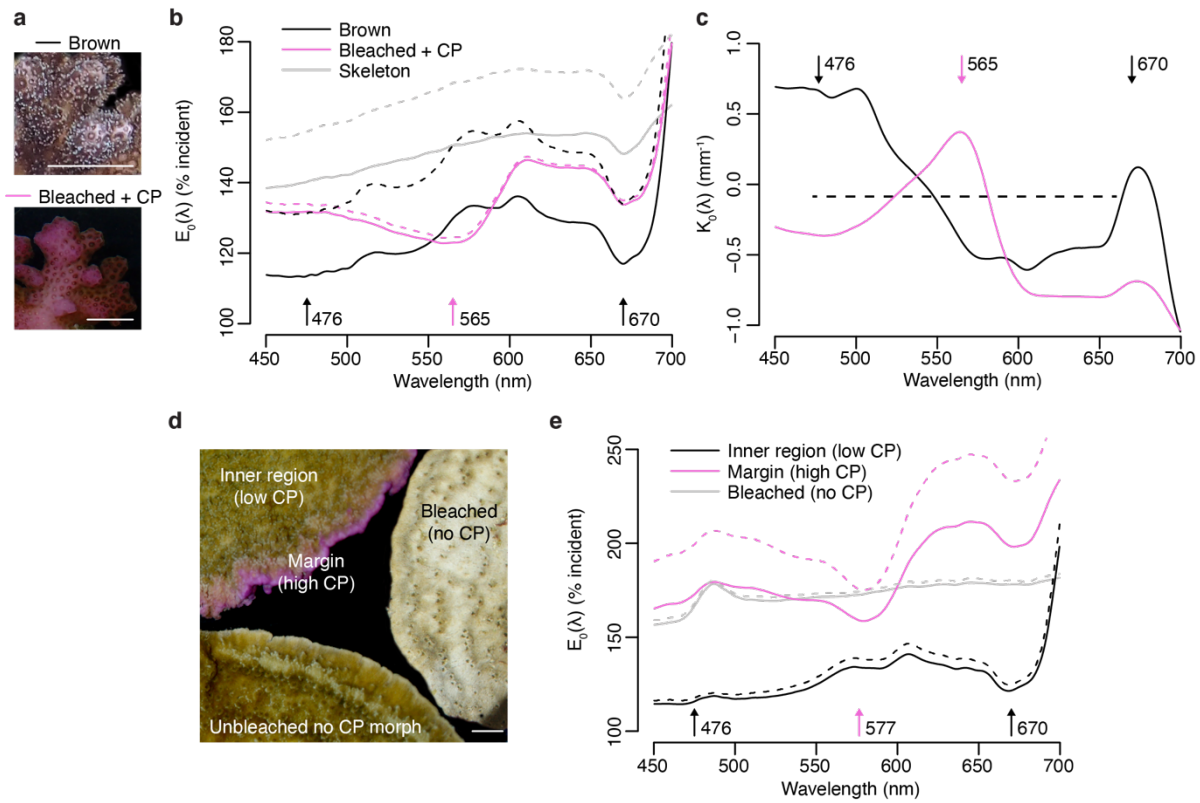

Figure 5. Effects of photoprotective chromoproteins on coral light environment. a) Representative photographs of unbleached brown and bleached pink *P. damicornis*. **b**) Spectral scalar irradiance ($E_0(\lambda)$) measurements at the coenosarc surface of unbleached brown *P. damicornis*, bleached *P. damicornis* with high CP content, and *P. damicornis* skeleton. **c**) Attenuation coefficient of $E_0(\lambda)$ for unbleached brown and bleached pink *P. damicornis*, calculated from surface to skeleton (tissue thickness = ~300 μm). **d**) Compilation of representative photographs of the unbleached high CP morph, unbleached no CP morph and bleached no CP morph of *M. foliosa*. **e**) Surface $E_0(\lambda)$ measurements of unbleached inner region (low CP), unbleached margin (high CP) and bleached no CP morph of *M. foliosa*. In **a** and **d**, scale bar = 5 mm. In **b** and **e**, mean (solid lines) ± s.d. (dashed lines), n=3. Arrows indicate peak absorption wavelength in nm for symbiont photosynthetic pigments (black) and CPs (pink).

While the pcRFPs and CPs examined in this study are characterised by very different optical properties, environmental regulation and ecological distribution, both coral host pigments can regulate internal light fluxes in the orange-red spectral range. Enhancement of this waveband can be a double-edged sword for corals; on one hand, poor absorption by photosynthetic pigments allows better penetration (Smith et al. 2017), which can be exploited by pcRFP-containing corals to illuminate deeper tissue areas under light limitation. On the other hand, light amplification in symbiont-free tissue produces excess irradiance in this waveband, which can cause photodamage unless counteracted by CP screening or other photoprotective mechanisms (Smith et al. 2013; Wijgerde et al. 2014; Wangpraseurt et al. 2017; Quick et al. 2018). Spectral regulation by GFP-like host pigments is thus a flexible

427 mechanism to achieve fine spectral regulation of the intra-tissue light field of corals, enabling
428 them to optimise light capture for their algal symbionts in response to environmental light
429 gradients. Future investigations into this diverse and ubiquitous protein family will likely
430 reveal further mechanisms through which the coral host supports light capture and facilitates
431 the photosymbiosis along the steep light gradients that characterise coral reef habitats.
432
433 **Materials and Methods**
434 Coral culture and aquarium set up
435 Coral colonies of *M. cavernosa*, *Echinophyllia* sp., *Pocillopora damicornis* and *Montipora*
436 *foliosa* were asexually propagated for >10 years in the experimental coral aquarium facility of
437 the Coral Reef Laboratory, National Oceanography Centre, Southampton, UK (D'Angelo and
438 Wiedenmann 2012).
439
440 Spectral scalar irradiance measurements
441 Microscale spectral light measurements were conducted as described in Wangpraseurt et al.
442 (2017) using scalar irradiance microsensors with a spherical tip diameter of 60 µm (Rickelt et
443 al. 2016) and connected to a fiber-optic spectrometer (QE65000, Ocean Optics, USA).
444 Microsensor profiles were performed from the coral skeleton upwards towards the tissue
445 surface in vertical increments of 20-100 µm using a motorized micromanipulator (Pyroscience
446 GmbH, Germany) controlled by dedicated software (Profix, Pyroscience GmbH, Germany).
447 The step size was adjusted according to the total coral tissue thickness with step sizes of 20
448 µm for *P. damicornis*, 70 µm for *M. cavernosa* and *Echinophyllia*. For *M. foliosa*, only surface
449 spectra were collected as the tissue was very thin (< 60 µm). Scalar irradiance measurements
450 were performed using vertical illumination from above, while the scalar irradiance microsensor
451 was inserted into coral tissue at an angle of 45° relative to the incident light (Fig. S1a). White
452 LED illumination was provided by a fiber-optic lamp (KL-1600 LED, Schott GmbH, Germany)
453 (Fig. S1a,b), producing 360-900 µmol photons m^{-2} s^{-1} at the measurement distance.
454 For *M. cavernosa* and *Echinophyllia*, we also measured the spatial distribution of emitted
455 fluorescence. For this, narrow-waveband excitation in the blue spectral range was provided
456 vertically incident by a xenon arc lamp equipped with a band-pass filter (Leica GFPplus filter,
457 λ=455-505nm, Fig. S1c) and scalar irradiance measurements in the 505-650 nm range were
458 used to estimate fluorescence emission. The light source output (455-505 nm) at the
459 measurement distance was 12-46 µmol photons m^{-2} s^{-1}. No emission filter was used on the
460 detector side as bleed-through of excitation light in this spectral range was minimal (<0.5%).
461 Scalar irradiance microsensor measurements were calibrated against a spectroradiometer
462 (MSC15, Gigahertz-Optik, Germany) by measuring the incident downwelling irradiance from

463 the white LED light source over a black light absorbing surface first with the microsensor in
464 water, then with the spectroradiometer at the same distance from the light source in air
465 (Wangpraseurt et al. 2012; Brodersen et al. 2014).
466
467 Induction of photoconversion and measurements of pcRFP-containing corals
468 We performed scalar irradiance measurements in *M. cavernosa* at different stages of
469 photoconversion to assess how near-UV driven photoconversion of the pcRFP pool affects
470 the symbiont light environment. We defined the stages of photoconversion by the relative
471 proportions of green (514 nm) and red (582 nm) fluorescence emission, measured with 455-
472 505 nm excitation at the colony surface. A 514:582 nm ratio >1 indicates a higher contribution
473 of the green chromophore (defined as *unconverted* coral), a ratio ~1 indicates substantial
474 contributions from both the green and the red chromophore (defined as *partially converted*
475 coral), and a ratio <1 indicates a higher contribution of the red chromophore (defined as
476 *converted* coral).
477 To obtain *unconverted* corals, we placed two colonies derived from fragmentation of the same
478 mother colony under green incident irradiance provided by LED strips (Lumiled Luxeon Rebel
479 Green, λ=530 nm, FWHM=60 nm; Fig. S2a) for 40 days. This treatment resulted in the
480 accumulation of the unconverted pcRFP (Leutenegger et al. 2007), evidenced by a 514:582
481 nm emission ratio >1. We then used one of these colonies to induce localised photoconversion
482 by illuminating the coral tissue surface (spot diameter 3 mm) with a xenon arc lamp of a
483 fluorescence microscope (Leica MZ10 equipped with a UV bandpass filter (λ=355 nm,
484 FWHM=55 nm; Fig. S2b) for 6 hours (Eyal et al. 2015); this waveband only partially overlaps
485 with the action spectrum of pcRFP photoconversion (Wiedenmann et al. 2004) and is therefore
486 less effective in inducing the photochemical reaction. In combination with the limited duration
487 of the exposure, the UV treatment resulted in a mix of unconverted and converted pcRFP, as
488 evidenced from the 514:582 nm ratio ~1 (*partially converted* coral). The second *M. cavernosa*
489 colony was exposed to near-UV irradiance provided by LED strips (Aquaray NUV, λ=412,
490 FWHM=18.5 nm; Fig. S2c) for 10 hours; this treatment induces rapid photoconversion of the
491 pcRFP pool (Bollati et al. 2017), resulting in a 514:582 nm emission ratio <1 (*converted* coral).
492 All photoconversion experiments were performed in a flow-through system at a water
493 temperature of 26°C regulated by a 25 W aquarium heater (Tunze).
494 We also assessed the contribution of fluorescence emission by pcRFPs to spectral scalar
495 irradiance against other GFP-like proteins by performing measurements on two morphs of
496 *Echinophyllia* sp.. Both morphs had been kept under broad spectrum illumination long term,
497 side by side in our mesocosm. The green morph contained a non-inducible GFP, while the

red morph contained a CFP and a highly converted pcRFP (green:red emission ratio <<1) (Alieva et al. 2008; Bollati et al. 2017; Smith et al. 2017).

Experimental bleaching and measurements of corals containing inducible CPs

To test how bleaching affects irradiance in corals containing inducible CPs, we performed measurements on healthy and bleached *P. damicornis* and *M. foliosa*. A *P. damicornis* colour morph capable of expressing a pink CP with absorption maximum at 565 nm (Dove et al. 1995; D'Angelo et al. 2008; Bollati et al. 2020) was bleached by exposure to 400 μmol photons m^{-2} s^{-1} of red LED light (Lumiled Luxeon Rebel Deep Red, λ=660 nm, FWHM=40 nm; Fig. S2d) for 7 days. This treatment induces bleaching without inducing the expression of the light-sensitive genes responsible for CP production (D'Angelo et al. 2008; Smith et al. 2013; Wijgerde et al. 2014; Bollati et al. 2020). Bleaching was confirmed by visual comparison with untreated specimens. Bleached fragments were then exposed to blue light (100 μmol photons m^{-2} s^{-1}; Lumiled Luxeon Rebel Royal Blue, λ=450 nm, FWHM=40 nm; Fig. S2e) for 20 days to stimulate upregulation of the pink CP, resulting in a "colourful bleaching" response (D'Angelo et al. 2008; Bollati et al. 2020) (Fig. S2). Alongside the bleached specimen, we performed spectral scalar irradiance measurements on i) a *P. damicornis* skeleton and ii) an unbleached brown morph of the same species, which expresses an inducible CFP but no CP.

For *M. foliosa*, we measured a morph capable of producing a CFP and a pink CP, with the latter accumulating in high concentrations at the colony margins (D'Angelo et al. 2012; Bollati et al. 2020). We compared this healthy, unbleached coral with a *M. foliosa* morph that does not produce CPs, bleached by phosphate starvation (Wiedenmann et al. 2013; Rosset et al. 2017; Bollati et al. 2020) after 65 days in our high nitrate / low phosphate mesocosm (D'Angelo and Wiedenmann 2012). Both colonies were kept under broad spectrum illumination (200 μmol photons m^{-2} s^{-1}; Aquamedic metal halide lamp).

Data processing

All spectral data were corrected for spectrometer dark noise readings obtained under dark conditions and calibrated against a spectroradiometer as described above. For spectral measurements performed under incident white light, the spectra were normalised to the incident irradiance as described previously (Wangpraseurt et al. 2012).

The spectral attenuation coefficient of scalar irradiance ($K_0(\lambda)$) was calculated from measurements obtained under white light following Kühl (2005):

$$K_0(\lambda) = \frac{\ln\left(\frac{E_0(\lambda)_1}{E_0(\lambda)_2}\right)}{z_2 - z_1}$$

where $E_0(\lambda)_1$ and $E_0(\lambda)_2$ are the spectral scalar irradiance measured at tissue depths z_1 and z_2. $K_0(\lambda)$ was calculated from surface to skeleton using the average tissue thickness (deduced from the mean number of equal steps performed by the micromanipulator from the skeleton to the upper tissue surface: 560 μm for *M. cavernosa*, 300 μm for *P. damicornis*).

For fluorescence emission measurements under blue excitation, integrated photon irradiance was calculated for different portions of the visible spectrum (incident: 455-505 nm; green emission: 505-560 nm; red emission: 560-650 nm) after converting spectral scalar irradiance to spectral photon scalar irradiance using Plancks equation (see (Lichtenberg et al. 2017)). Integrated photon irradiance over the same incident (455-505 nm) and red (560-650 nm) spectral ranges was also calculated for a dataset of field spectral scalar irradiance collected from Eilat, Israel (Eyal et al. 2015) and for a dataset of spectral scalar irradiance simulated from surface measurements collected in the Bahamas (Lesser et al. 2009).

Acknowledgements

This project was supported by the European Union's Horizon 2020 research and innovation programme (702911-BioMIC-FUEL, D.W.), the Gordon and Betty More Foundation (grant GBM 9325 to D.W. & grant GBMF9206 https://doi.org/10.37807/GBMF9206 to MK) and the Natural Environment Research Council (grant number NE/S003533/2 to JW and CDA).

Data availability

Data used in this study is available from https://doi.org/10.5061/dryad.0gb5mkm1z

References

Aihara Y, Maruyama S, Baird AH, Iguchi A, Takahashi S, Minagawa J (2019) Green fluorescence from cnidarian hosts attracts symbiotic algae. Proc Natl Acad Sci 116:2118–2123

Alieva NO, Konzen KA, Field SF, Meleshkevitch EA, Hunt ME, Beltran-Ramirez V, Miller DJ, Wiedenmann J, Salih A, Matz M V (2008) Diversity and evolution of coral fluorescent proteins. PLoS One 3:e2680

Ando R, Hama H, Yamamoto-Hino M, Mizuno H, Miyawaki A (2002) An optical marker based on the UV-induced green-to-red photoconversion of a fluorescent protein. Proc Natl Acad Sci 99:12651–12656

Anthony KRN, Hoegh-Guldberg O (2003) Variation in coral photosynthesis, respiration and growth characteristics in contrasting light microhabitats: An analogue to plants in forest gaps and understoreys? Funct Ecol 17:246–259

Anthony KRN, Hoogenboom MO, Connolly SR (2005) Adaptive variation in coral geometry and the optimization of internal colony light climates. Funct Ecol 19:17–26

Ben-Zvi O, Wangpraseurt D, Bronstein O, Eyal G, Loya Y (2021) Photosynthesis and bio-optical properties of fluorescent mesophotic corals. Front Mar Sci 8:1–12

Bollati E, D'Angelo C, Alderdice R, Pratchett M, Ziegler M, Wiedenmann J (2020) Optical feedback loop involving dinoflagellate symbiont and scleractinian host drives colorful coral bleaching. Curr Biol 30:1–13

Bollati E, Plimmer D, D'Angelo C, Wiedenmann J (2017) FRET-mediated long-range wavelength transformation by photoconvertible fluorescent proteins as an efficient mechanism to generate orange-red light in symbiotic deep water corals. Int J Mol Sci 18:1174

Brakel W (1979) Small-scale spatial variation in light available to coral reef benthos: Quantum irradiance measurements from a Jamaican reef. Bull Mar Sci 29:406–413

Brodersen KE, Lichtenberg M, Ralph PJ, Kühl M, Wangpraseurt D (2014) Radiative energy budget reveals high photosynthetic efficiency in symbiont-bearing corals. J R Soc

582 Interface 11:
583 D'Angelo C, Denzel A, Vogt A, Matz M V., Oswald F, Salih A, Nienhaus GU, Wiedenmann J
584 (2008) Blue light regulation of host pigment in reef-building corals. Mar Ecol Prog Ser
585 364:97–106
586 D'Angelo C, Smith EG, Oswald F, Burt J, Tchernov D, Wiedenmann J (2012) Locally
587 accelerated growth is part of the innate immune response and repair mechanisms in
588 reef-building corals as detected by green fluorescent protein (GFP)-like pigments. Coral
589 Reefs 31:1045–1056
590 D'Angelo C, Wiedenmann J (2012) An experimental mesocosm for long-term studies of reef
591 corals. J Mar Biol Assoc United Kingdom 92:769–775
592 Dove SG, Takabayashi M, Hoegh-Guldberg O (1995) Isolation and partial characterization of
593 the pink and blue pigments of pocilloporid and acroporid corals. Biol Bull 189:288–297
594 Einbinder S, Mass T, Brokovich E, Dubinsky Z, Erez J, Tchernov D (2009) Changes in
595 morphology and diet of the coral *Stylophora pistillata* along a depth gradient. Mar Ecol
596 Prog Ser 381:167–174
597 Enríquez S, Méndez ER, Hoegh-Guldberg O, Iglesias-Prieto R (2017) Key functional role of
598 the optical properties of coral skeletons in coral ecology and evolution. Proc R Soc
599 London B Biol Sci 284:
600 Enríquez S, Méndez ER, Iglesias-Prieto R (2005) Multiple scattering on coral skeletons
601 enhances light absorption by symbiotic algae. Limnol Oceanogr 50:1025–1032
602 Eyal G, Wiedenmann J, Grinblat M, D'Angelo C, Kramarsky-Winter E, Treibitz T, Ben-Zvi O,
603 Shaked Y, Smith TB, Harii S, Denis V, Noyes T, Tamir R, Loya Y (2015) Spectral
604 diversity and regulation of coral fluorescence in a mesophotic reef habitat in the Red
605 Sea. PLoS One 10:e0128697
606 Falkowski PG, Dubinsky Z (1981) Light-shade adaptation of *Stylophora pistillata*, a
607 hermatypic coral from the Gulf of Eilat. Nature 289:172–174
608 Field S, Bulina M, Kelmanson I, Bielawski J, Matz M (2006) Adaptive evolution of
609 multicolored fluorescent proteins in reef-building corals. J Mol Evol 62:332–339
610 Fisher R, O'Leary RA, Low-Choy S, Mengersen K, Knowlton N, Brainard RE, Caley MJ
611 (2015) Species richness on coral reefs and the pursuit of convergent global estimates.
612 Curr Biol 25:500–505
613 Gittins JR, D'Angelo C, Oswald F, Edwards RJ, Wiedenmann J (2015) Fluorescent protein-
614 mediated colour polymorphism in reef corals: multicopy genes extend the
615 adaptation/acclimatization potential to variable light environments. Mol Ecol 24:453–465
616 Gorbunov MY, Kolber ZS, Lesser MP, Falkowski PG (2001) Photosynthesis and
617 photoprotection in symbiotic corals. Limnol Oceanogr 46:75–85
618 Helmuth BST, Timmerman BEH, Sebens KP (1997) Interplay of host morphology and

symbiont microhabitat in coral aggregations. Mar Biol 130:1–10
Hoegh-Guldberg O, Jones RJ (1999) Photoinhibition and photoprotection in symbiotic dinoflagellates from reef-building corals. Mar Ecol Prog Ser 183:73–86
Hoogenboom MO, Connolly SR, Anthony KRN (2008) Interactions between morphological and physiological plasticity optimize energy acquisition in corals. Ecology 89:1144–1154
Id HY, Koike K, Shinzato C, Jimbo M, Suzuki G (2021) Can *Acropora tenuis* larvae attract native Symbiodiniaceae cells by green fluorescence at the initial establishment of symbiosis? PLoS One 16:e0252514
Jiang J, Zhang H, Kang Y, Bina D, Lo CS, Blankenship RE (2012) Characterization of the peridinin-chlorophyll a-protein complex in the dinoflagellate *Symbiodinium*. Biochim Biophys Acta - Bioenerg 1817:983–989
Jimenez IM, Larkum AWD, Ralph PJ, Kühl M (2012) *In situ* thermal dynamics of shallow water corals is affected by tidal patterns and irradiance. Mar Biol 159:1773–1782
Kahng SE, Akkaynak D, Shlesinger T, Hochberg EJ, Wiedenmann J, Tamir R, Tchernov D (2019) Light, temperature, photosynthesis, heterotrophy, and the lower depth limits of mesophotic coral ecosystems. In: Loya Y., Puglise K.A., Bridge T.C.L. (eds) Mesophotic Coral Ecosystems. Springer International Publishing, Cham, pp 801–828
Kaniewska P, Magnusson SH, Anthony KRN, Reef R, Kühl M, Hoegh-Guldberg O (2011) Importance of macro- versus microstructure in modulating light levels inside coral colonies. J Phycol 47:846–860
Kirk JTO (1994) Light and photosynthesis in aquatic ecosystems. Cambridge University Press,
Kleypas JA, McManu JW, Mene LAB (1999) Environmental limits to coral reef development: Where do we draw the line? Am Zool 39:146–159
Kramer N, Guan J, Mumm K, Wangpraseurt D, Loya Y Functional morphological-traits optimize light-harvesting in stony corals.
Kramer N, Tamir R, Ben-Zvi O, Jacques SL, Loya Y, Wangpraseurt D (2020) Light-harvesting in mesophotic corals is powered by a spatially efficient photosymbiotic system between coral host and microalgae. bioRxiv
Kühl M (2005) Optical microsensors for analysis of microbial communities. In: Leadbetter J.R. (eds) Environmental Microbiology. Academic Press, pp 166–199
Kühl M, Cohen Y, Dalsgaard T, Jorgensen BB, Revsbech NP (1995) Microenvironment and photosynthesis of zooxanthellae in scleractinian corals studied with microsensors for 0_2, pH and light. Mar Ecol Prog Ser 117:159-172.1995
Lesser MP, Slattery M, Leichter JJ (2009) Ecology of mesophotic coral reefs. J Exp Mar Bio Ecol 375:1–8

656 Lesser MP, Slattery M, Stat M, Ojimi M, Gates RD, Grottoli A (2010) Photoacclimatization by
657 the coral *Montastraea cavernosa* in the mesophotic zone: light, food, and genetics.
658 Ecology 91:990–1003
659 Leutenegger A, D'Angelo C, Matz M V, Denzel A, Oswald F, Salih A, Nienhaus GU,
660 Wiedenmann J (2007) It's cheap to be colorful. FEBS J 274:2496–2505
661 Lichtenberg M, Brodersen KE, Kühl M (2017) Radiative energy budgets of phototrophic
662 surface-associated microbial communities and their photosynthetic efficiency under
663 diffuse and collimated light. Front Microbiol 8:1–17
664 López-Londoño T, Galindo-Martínez CT, Gómez-Campo K, González-Guerrero LA, Roitman
665 S, Pollock FJ, Pizarro V, López-Victoria M, Medina M, Iglesias-Prieto R (2021)
666 Physiological and ecological consequences of the water optical properties degradation
667 on reef corals. Coral Reefs 40:1243–1256
668 Lyndby NH, Kuhl M, Wangpraseurt D (2016) Heat generation and light scattering of green
669 fluorescent protein-like pigments in coral tissue. Sci Rep 6:26599
670 Marcelino LA, Westneat MW, Stoyneva V, Henss J, Rogers JD, Radosevich A, Turzhitsky V,
671 Siple M, Fang A, Swain TD, Fung J, Backman V (2013) Modulation of light-
672 enhancement to symbiotic algae by light-scattering in corals and evolutionary trends in
673 bleaching. PLoS One 8:e61492
674 Matz M V, Fradkov AF, Labas YA, Savitsky AP, Zaraisky AG, Markelov ML, Lukyanov SA
675 (1999) Fluorescent proteins from nonbioluminescent Anthozoa species. Nat Biotechnol
676 17:969–973
677 de Mooij T, de Vries G, Latsos C, Wijffels RH, Janssen M (2016) Impact of light color on
678 photobioreactor productivity. Algal Res 15:32–42
679 Muscatine L (1990) The role of sybiotic algae in carbon and energy flux in coral reefs. In:
680 Dubinsky Z. (eds) Ecosystems of the World, 25. Coral Reefs. Elsevier, Amsterdam, pp
681 75–87
682 Nienhaus GU, Wiedenmann J (2009) Structure, dynamics and optical properties of
683 fluorescent proteins: perspectives for marker development. ChemPhysChem 10:1369–
684 1379
685 Nir O, Gruber DF, Einbinder S, Kark S, Tchernov D (2011) Changes in scleractinian coral
686 *Seriatopora hystrix* morphology and its endocellular *Symbiodinium* characteristics along
687 a bathymetric gradient from shallow to mesophotic reef. Coral Reefs 30:1089–1100
688 Oswald F, Schmitt F, Leutenegger A, Ivanchenko S, D'Angelo C, Salih A, Maslakova S,
689 Bulina M, Schirmbeck R, Nienhaus GU, Matz M V, Wiedenmann J (2007) Contributions
690 of host and symbiont pigments to the coloration of reef corals. FEBS J 274:1102–1122
691 Parkins SKT, Murthy S, Picioreanu C, Kühl M (2021) Multiphysics modelling of photon, mass
692 and heat transfer in coral microenvironments. J R Soc Interface In Press:

693 Quick C, D'Angelo C, Wiedenmann J (2018) Trade-offs associated with photoprotective
694 Green Fluorescent Protein expression as potential drivers of balancing selection for
695 color polymorphism in reef corals. Front Mar Sci 5:1–11
696 Ralph PJ, Gademann R, Larkum AWD, Kühl M (2002) Spatial heterogeneity in active
697 chlorophyll fluorescence and PSII activity of coral tissues. Mar Biol 141:639–646
698 Rickelt LF, Lichtenberg M, Trampe ECL, Kühl M (2016) Fiber-optic probes for small-scale
699 measurements of scalar irradiance. Photochem Photobiol 92:331–342
700 Rosset S, Wiedenmann J, Reed AJ, D'Angelo C (2017) Phosphate deficiency promotes
701 coral bleaching and is reflected by the ultrastructure of symbiotic dinoflagellates. Mar
702 Pollut Bull 118:180–187
703 Rouzé H, Galand PE, Medina M, Bongaerts P, Pichon M, Pérez-Rosales G, Torda G, Moya
704 A, Bardout G, Périé-Bardout E, Marivint E, Lagarrigue G, Leblond J, Gazzola F, Pujolle
705 S, Mollon N, Mittau A, Fauchet J, Paulme N, Pete R, Peyrusse K, Ferucci A, Magnan A,
706 Horlaville M, Breton C, Gouin M, Markocic T, Jubert I, Herrmann P, Raina JB, Hédouin
707 L (2021) Symbiotic associations of the deepest recorded photosynthetic scleractinian
708 coral (172 m depth). ISME J 15:1564–1568
709 Salih A, Larkum A, Cox G, Kühl M, Hoegh-Guldberg O (2000) Fluorescent pigments in
710 corals are photoprotective. Nature 408:850–853
711 Scheufen T, Iglesias-Prieto R, Enríquez S (2017) Changes in the number of symbionts and
712 *Symbiodinium* cell pigmentation modulate differentially coral light absorption and
713 photosynthetic performance. Front Mar Sci 4:1–17
714 Schlichter D, Meier U, Fricke HW (1994) Improvement of photosynthesis in zooxanthellate
715 corals by autofluorescent chromatophores. Oecologia 99:124–131
716 Shagin DA, Barsova E V, Yanushevich YG, Fradkov AF, Lukyanov KA, Labas YA,
717 Semenova TN, Ugalde JA, Meyers A, Nunez JM, Widder EA, Lukyanov SA, Matz M V
718 (2004) GFP-like proteins as ubiquitous metazoan superfamily: evolution of functional
719 features and structural complexity. Mol Biol Evol 21:841–850
720 Shimomura O, Johnson FH, Saiga Y (1962) Extraction, purification and properties of
721 aequorin, a bioluminescent protein from the luminous hydromedusan, *Aequorea*. J Cell
722 Comp Physiol 59:223–239
723 Smith EG, D'Angelo C, Salih A, Wiedenmann J (2013) Screening by coral green fluorescent
724 protein (GFP)-like chromoproteins supports a role in photoprotection of zooxanthellae.
725 Coral Reefs 32:463–474
726 Smith EG, D'Angelo C, Sharon Y, Tchernov D, Wiedenmann J (2017) Acclimatization of
727 symbiotic corals to mesophotic light environments through wavelength transformation
728 by fluorescent protein pigments. Proc R Soc London B Biol Sci 284:
729 Szabó M, Wangpraseurt D, Tamburic B, Larkum AWD, Schreiber U, Suggett DJ, Kühl M,

730 Ralph PJ (2014) Effective light absorption and absolute electron transport rates in the
731 coral *Pocillopora damicornis*. Plant Physiol Biochem 83:159–167
732 Tamir R, Ben-Zvi O, Eyal G, Kramer N, Loya Y (2020) Reciprocal-transplantation between
733 shallow and mesophotic stony corals. Mar Environ Res 161:
734 Tamir R, Eyal G, Kramer N, Laverick JH, Loya Y (2019) Light environment drives the
735 shallow-to-mesophotic coral community transition. Ecosphere 10:
736 Titlyanov EA, Titlyanova T V, Yamazato K, van Woesik R (2001) Photo-acclimation
737 dynamics of the coral *Stylophora pistillata* to low and extremely low light. J Exp Mar Bio
738 Ecol 263:211–225
739 Todd PA (2008) Morphological plasticity in scleractinian corals. Biol Rev 83:315–337
740 Ugalde JA, Chang BSW, Matz M (2004) Evolution of coral pigments recreated. Science (80-
741) 305:1433
742 Veal CJ, Carmi M, Dishon G, Sharon Y, Michael K, Tchernov D, Hoegh-Guldberg O, Fine M
743 (2010) Shallow-water wave lensing in coral reefs: a physical and biological case study.
744 J Exp Biol 213:4304–4312
745 Vogelmann TC, Evans JR (2002) Profiles of light absorption and chlorophyll within spinach
746 leaves from chlorophyll fluorescence. Plant, Cell Environ 25:1313–1323
747 Wangpraseurt D, Holm JB, Larkum AWD, Pernice M, Ralph PJ, Suggett DJ, Kühl M (2017)
748 *In vivo* microscale measurements of light and photosynthesis during coral bleaching:
749 Evidence for the optical feedback loop? Front Microbiol 8:59
750 Wangpraseurt D, Jacques S, Lyndby N, Holm JB, Pages CF, Kühl M (2019) Microscale light
751 management and inherent optical properties of intact corals studied with optical
752 coherence tomography. J R Soc Interface 16:20180567
753 Wangpraseurt D, Jacques SL, Petrie T, Kühl M (2016a) Monte Carlo modeling of photon
754 propagation reveals highly scattering coral tissue. Front Plant Sci 7:1404
755 Wangpraseurt D, Larkum AWD, Franklin J, Szabó M, Ralph PJ, Kühl M (2014a) Lateral light
756 transfer ensures efficient resource distribution in symbiont-bearing corals. J Exp Biol
757 217:489–98
758 Wangpraseurt D, Larkum AWD, Ralph PJ, Kühl M (2012) Light gradients and optical
759 microniches in coral tissues. Front Microbiol 3:316
760 Wangpraseurt D, Pernice M, Guagliardo P, Kilburn MR, Clode PL, Polerecky L, Kühl M
761 (2016b) Light microenvironment and single-cell gradients of carbon fixation in tissues of
762 symbiont-bearing corals. ISME J 10:788–792
763 Wangpraseurt D, Polerecky L, Larkum AWD, Ralph PJ, Nielsen DA, Pernice M, Kühl M
764 (2014b) The *in situ* light microenvironment of corals. Limnol Oceanogr 59:917–926
765 Wangpraseurt D, You S, Azam F, Jacucci G, Gaidarenko O, Hildebrand M, Kühl M, Smith
766 AG, Davey MP, Smith A, Deheyn DD, Chen S, Vignolini S (2020) Bionic 3D printed

corals. Nat Commun 11:

Wiedenmann J, D'Angelo C, Smith EG, Hunt AN, Legiret F-E, Postle AD, Achterberg EP (2013) Nutrient enrichment can increase the susceptibility of reef corals to bleaching. Nat Clim Chang 3:160–164

Wiedenmann J, Ivanchenko S, Oswald F, Schmitt F, Röcker C, Salih A, Spindler K-D, Nienhaus GU (2004) EosFP, a fluorescent marker protein with UV-inducible green-to-red fluorescence conversion. Proc Natl Acad Sci U S A 101:15905–15910

Wijgerde T, van Melis A, Silva CIF, Leal MC, Vogels L, Mutter C, Osinga R (2014) Red light represses the photophysiology of the scleractinian coral *Stylophora pistillata*. PLoS One 9:e92781

Willis BL (1985) Phenotypic plasticity versus phenotypic stability in the reef corals *Turbinaria mesenterina* and *Pavona cactus*. 4:107–112

Supplementary Information file

Green fluorescent protein-like pigments optimize the internal light environment in symbiotic reef building corals

Elena Bollati[1,2,3*], Niclas H. Lyndby[2,4], Cecilia D'Angelo[1], Michael Kühl[2,5], Jörg Wiedenmann[1] & Daniel Wangpraseurt[6,7,8*]

[1]Coral Reef Laboratory, School of Ocean and Earth Science, University of Southampton, United Kingdom
[2]Marine Biology Section, Department of Biology, University of Copenhagen, Strandpromenaden 5, DK-3000 Helsingør, Denmark
[3]Department of Biological Sciences, National University of Singapore, 16 Science Drive 4, Singapore 117558
[4]Laboratory for Biological Geochemistry, School of Architecture, Civil and Environmental Engineering, Ecole Polytechnique Fédérale de Lausanne (EPFL), CH-1015 Lausanne, Switzerland
[5]Climate Change Cluster, University of Technology Sydney, Ultimo, NSW 2007, Australia
[6]Department of NanoEngineering, UC San Diego, USA
[7]Marine Biological Research Division, Scripps Institution of Oceanography, UC San Diego, USA
[8]Bioinspired photonics group, Department of Chemistry, University of Cambridge, UK

*Correspondence: dwangpraseurt@ucsd.edu, elena.bollati@bio.ku.dk

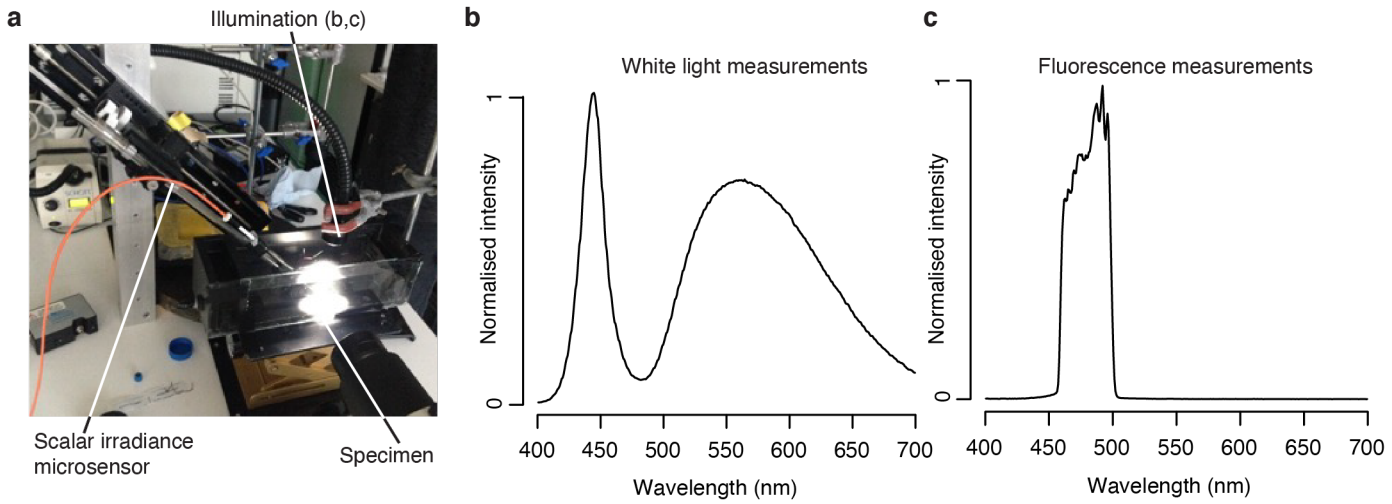

Figure S1. The scalar irradiance measurement set up (**a**) and spectra of the two light sources used for measurement (KL-1600 LED, **b**; xenon arc lamp + GFPplus filter, **c**)

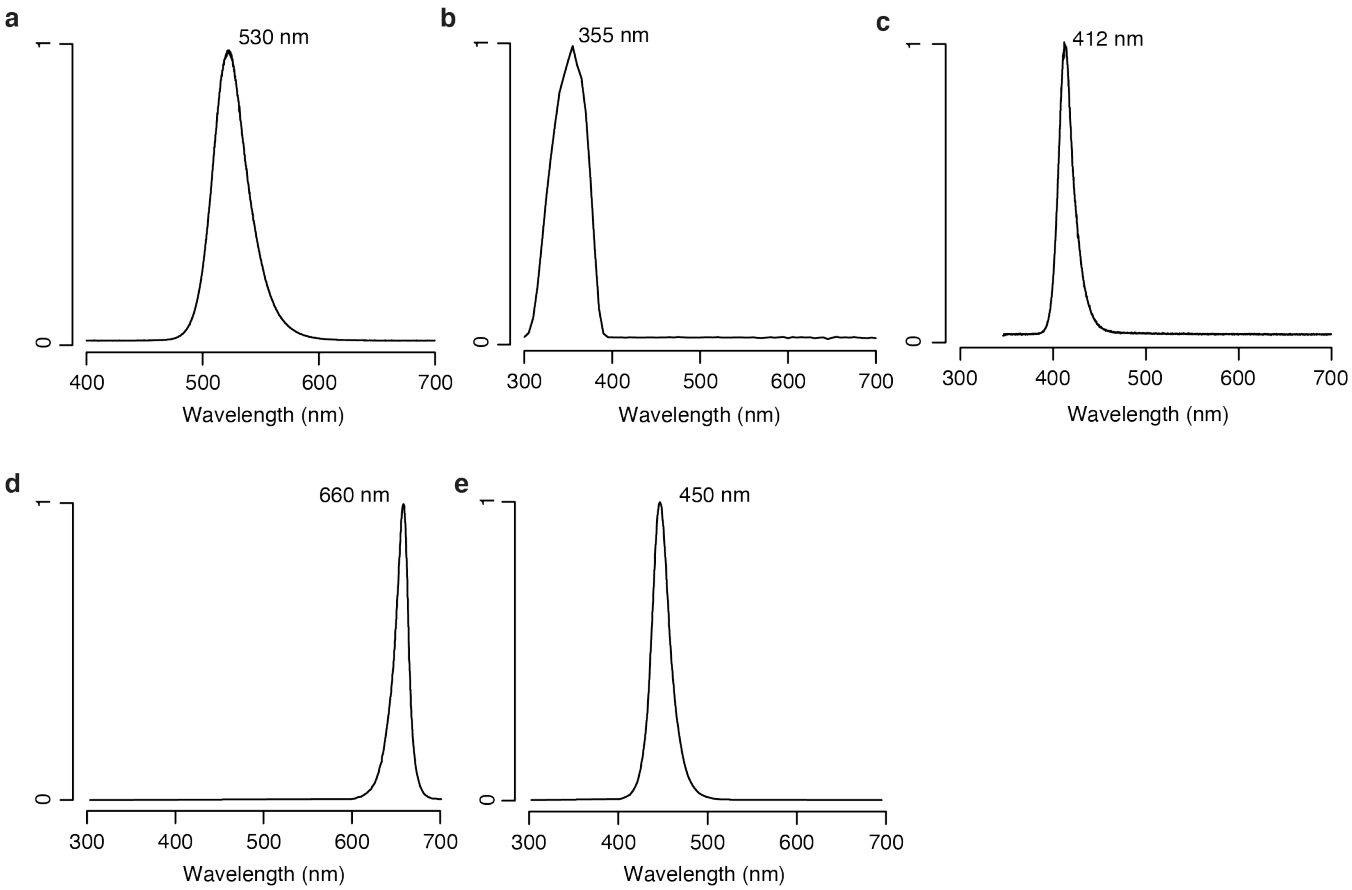

Figure S2. Spectra of light sources used for photoconversion (**a**-**c**) and bleaching (**d**,**e**) experiments (**a**, Lumiled Luxeon Rebel Green; **b**, xenon arc lamp + UV bandpass; **c**, Aquaray NUV; **d**, Lumiled Luxeon Rebel Deep Red; **e**, Lumiled Luxeon Rebel Royal Blue)

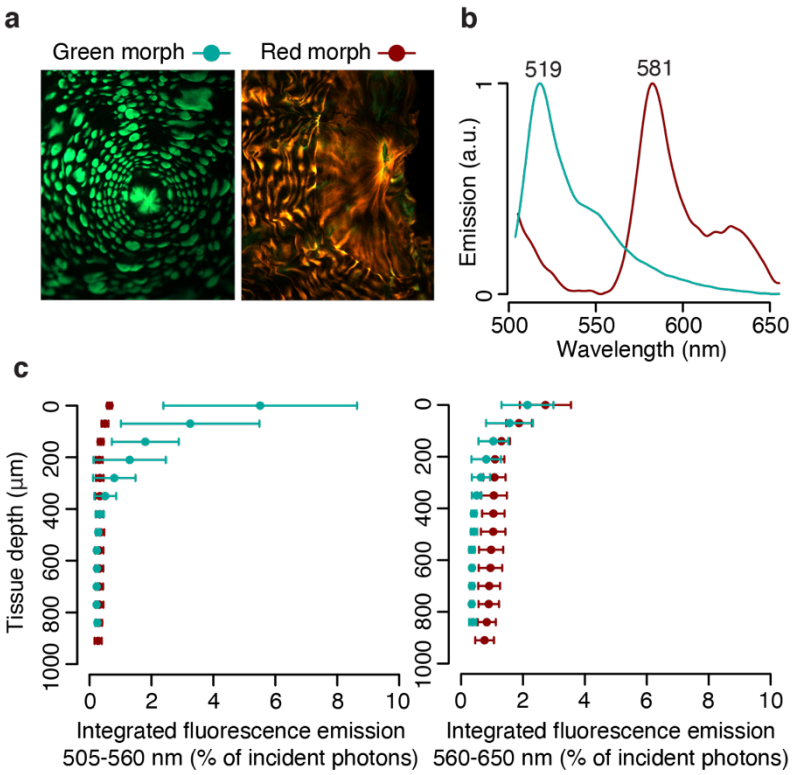

Figure S3. Photon scalar irradiance in the tissue of green and red morphs of *Echinophyllia*. **a**) Fluorescence micrographs (**a**) and surface fluorescence emission (**b**) of green and red morphs. **c**) Integrated green (505-560 nm) and red (560-650 nm) fluorescence emission along a tissue depth profile, measured under blue excitation (455-505 nm, Fig. S1). Spheres show means ± s.d., n=3.

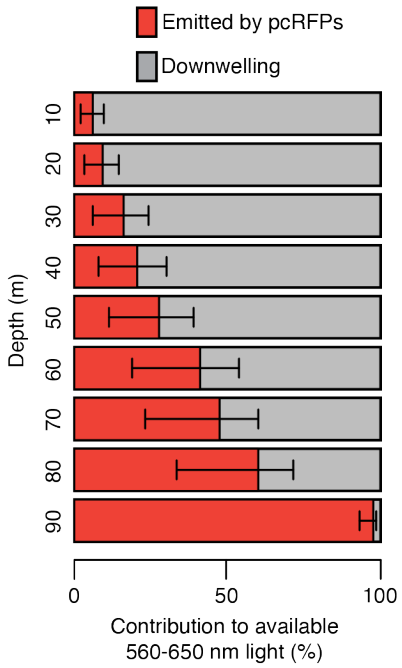

Figure S4. Relative contribution of fluorescence emission by pcRFPs and downwelling irradiance to the total 560-650 nm light available to pcRFP-containing corals along a depth gradient in the Bahamas (modelled irradiance data from ref [13]).

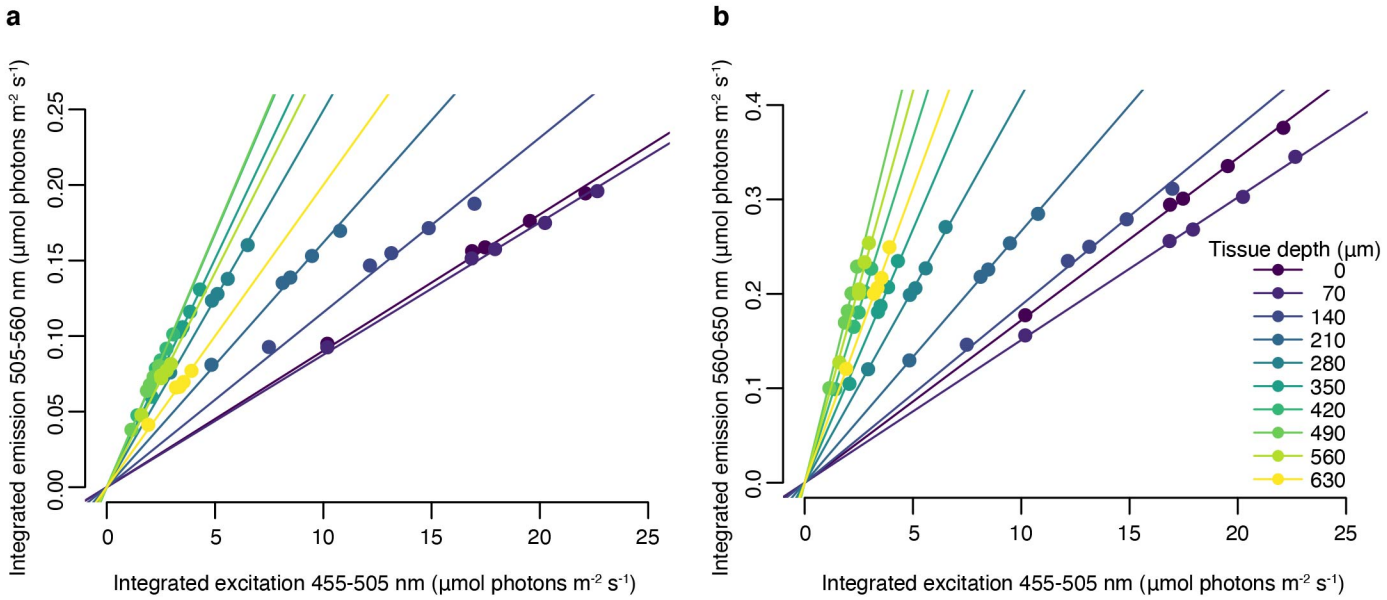

Figure S5. Relationship between blue (455-505 nm) excitation light photon irradiance and emitted green (505-560 nm, **a**) or red (560-650 nm, **b**) fluorescence at 10 tissue depths, obtained with a set of neutral density filters. Trendlines represent fitted linear regression (adjusted $p<0.05$, table S1).

<u>Incident intensity calibration (Fig. S5 Supplementary Methods)</u>

To determine whether the relationship between excitation light intensity and emitted fluorescence was linear within our measurement range, we performed a calibration profile on a *converted M. cavernosa* sample using a set of neutral density filters. At each depth, we collected fluorescence emission measurements under 455-505 nm excitation with five combinations of neutral density filters placed between the excitation light and the specimen. For each measurement, we then calculated the integrated photon scalar irradiance in the incident range (455-505 nm), the integrated green fluorescence emission (505-560 nm, fig. S5a) and the integrated red fluorescence emission (560-610 nm, fig. S5b). A linear regression was fitted for each tissue depth and each chromophore, with intercept set to zero (Fig. S5); p-values were corrected for multiple testing using the Bonferroni adjustment.

Table S1. Linear regression results for Fig. S5.

Green (505-560 nm) fluorescence emission

Depth	Slope	Std Error	t value	R^2 adjusted	P	Adjusted P
0	0.00902626	9.03E-05	99.9875929	0.99950008	6.00E-08	6.00E-07
70	0.0087601	7.62E-05	114.967832	0.99962183	3.43E-08	3.43E-07
140	0.01156811	0.00021343	54.2017461	0.99830038	6.94E-07	6.94E-06
210	0.01619148	0.00017715	91.4024378	0.9994018	8.59E-08	8.59E-07
280	0.02494033	0.00019703	126.581943	0.99968803	2.34E-08	2.34E-07
350	0.03021069	0.00018083	167.069327	0.99982089	7.70E-09	7.70E-08
420	0.03351092	0.0003004	111.554686	0.99959834	3.87E-08	3.87E-07
490	0.033718	0.00022538	149.603347	0.99977664	1.20E-08	1.20E-07
560	0.02842214	0.00042339	67.1300277	0.99889146	2.95E-07	2.95E-06
630	0.01999956	0.00028305	70.6577889	0.9989993	2.40E-07	2.40E-06

Red (560-650 nm) fluorescence emission

Depth	Slope	Std Error	t value	R^2 adjusted	P	Adjusted P
0	0.01719483	8.20E-05	209.593244	0.99988619	3.11E-09	3.11E-08
70	0.01510699	6.92E-05	218.286085	0.99989507	2.64E-09	2.64E-08
140	0.01881416	0.00019939	94.3604722	0.9994387	7.56E-08	7.56E-07
210	0.0266481	8.29E-05	321.256566	0.99995155	5.63E-10	5.63E-09
280	0.04096949	0.00025024	163.718467	0.99981349	8.35E-09	8.35E-08
350	0.05367283	0.00046253	116.040816	0.99962879	3.31E-08	3.31E-07
420	0.07300642	0.00047553	153.525421	0.9997879	1.08E-08	1.08E-07
490	0.09251997	0.00093074	99.4042684	0.99949419	6.14E-08	6.14E-07
560	0.08291338	0.00118633	69.8904363	0.99897723	2.51E-07	2.51E-06
630	0.06235948	0.00053652	116.22921	0.99962999	3.29E-08	3.29E-07